# Cathodic Disintegration as an Easily Scalable Method for the Production of Sn- and Pb-Based Catalysts for CO2 Reduction

Pavesi, D.; van de Poll, R.C.J.; Krasovic, J.L.; Figueiredo, M.; Gruter, G.-J.M.; Koper, M.T.M.; Schouten, K.J.P.

**DOI**
10.1021/acssuschemeng.0c04875

**Publication date**
2020

**Document Version**
Final published version

**Published in**
ACS Sustainable Chemistry & Engineering

ACS Sustainable Chemistry & Engineering

pubs.acs.org/journal/ascecg

Research Article

# Cathodic Disintegration as an Easily Scalable Method for the Production of Sn- and Pb-Based Catalysts for $CO_2$ Reduction

Davide Pavesi,* Rim C. J. van de Poll, Julia L. Krasovic, Marta Figueiredo, Gert-Jan M. Gruter, Marc T. M. Koper, and Klaas Jan P. Schouten*

Cite This: *ACS Sustainable Chem. Eng.* 2020, 8, 15603−15610

Read Online

ACCESS | Metrics & More | Article Recommendations | Supporting Information

**ABSTRACT:** $CO_2$ electroreduction to formate powered by renewable energy is an attractive strategy to recycle air-based carbon. At the moment, the electrode materials showing high selectivity for formate at high current density are post transition metals such as In, Sn, Bi, and Pb. Scaling up the $CO_2$ electroreduction technology to industrial size requires, among other things, cheap and clean methods to produce cathode materials in the form of particles to fabricate the square meters of the electrode surface area needed for the industrial electrolyzers. We show here that it is possible to easily produce catalytic powders based on Sn and Pb via a process known as cathodic disintegration, driving the reaction with electric power and avoiding the use of organic solvents, stabilizers, and reducing agents. The catalysts produced with this method are highly selective for the reduction of $CO_2$ to formate and show promise for use in industrial electrolyzers. Moreover, the process of cathodic disintegration is quick and clean, it has a high atom efficiency, it uses dilute aqueous electrolytes as solvents, and it has the possibility to be driven by renewable energy.

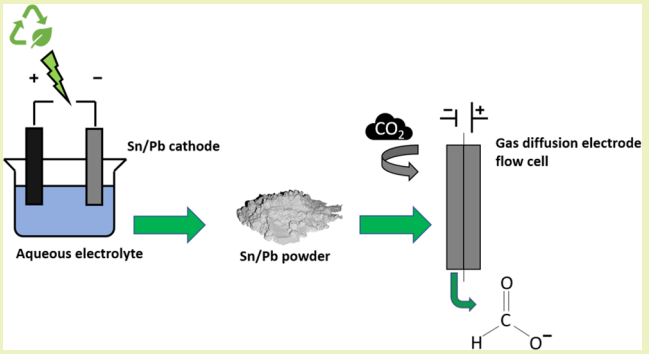


**KEYWORDS:** *cathodic disintegration, cathodic corrosion, nanoparticles, electrocatalysis, $CO_2$ reduction*

## INTRODUCTION

The electrocatalytic conversion of $CO_2$ is of considerable interest nowadays due to the possibility of using energy from renewable sources to convert this ubiquitous and rather inert waste product to value-added chemicals and fuels.[1] The reaction can yield several products such as CO, methane, ethylene, and formic acid. Among these, formic acid is of particular interest because of its possible use as a liquid fuel precursor and hydrogen carrier for fuel cell applications[2] and because of the existing market as a preservative in animal feed and in the production of leather. The formic acid salt (formate) can be used as a precursor to C2 chemicals such as oxalic acid, glyoxylic acid, and glycolic acid, thus enabling further conversions.[3,4] The small number of electrons (two) needed for the conversion of $CO_2$ to formic acid and formate, together with the high atom efficiency, make this conversion one of the economically most promising electrocatalytic conversions. Typically, catalysts based on metals such as Sn, In, Pb, Hg, and Bi are used, as they show high catalytic selectivity to convert $CO_2$ into formate.[5] High productivities are obtained using gas diffusion electrode (GDE) configurations because GDEs allow us to overcome mass transport limitations arising from the low solubility of $CO_2$, which is a common drawback to achieve high reaction yields at high current densities.

In this work, we study a relatively unexplored method for the production of metal catalyst particles: cathodic disintegration of Sn and Pb.[6,7] During the process, particles are produced directly upon cathodic polarization of metals in aqueous electrolytes, and it is possible to produce catalysts that can be readily coated on a GDE to catalyze the electrochemical conversion of $CO_2$ to formate. The method avoids the use of surfactants, stabilizers, organic solvents, reducing agents, and expensive chemicals, which can hamper the industrial use of catalysts prepared by other common reduction−deposition methods.[8] In addition, the method is extremely quick.

Using cathodic disintegration, we produced catalysts based on unsupported particles of Sn, Pb, and a Sn50Pb50 alloy. These catalysts were tested by applying them as an ink to a 10 $cm^2$ GDE and the results indicate that they perform well in industrial conditions.

Moreover, we tested the possibility to directly make carbon-supported Sn particles using cathodic disintegration, inves-

Received: July 2, 2020
Revised: September 7, 2020
Published: September 24, 2020

tigating the effect of different applied currents during the disintegration process on the morphological characteristics of the catalyst and tested these carbon-supported catalysts in a GDE flow cell, benchmarking them against a carbon-supported Sn catalyst prepared by a simple chemical reduction method available in the literature.[9] The best performing catalyst prepared by cathodic disintegration outperforms the benchmark in selectivity (average faradic yield of benchmark 73 vs 98% for our cathodic disintegration catalyst).

These findings open up the possibility to quickly produce catalysts in the form of a powder (with a high surface area and easily transferrable to GDEs) based on Pb, Sn, their alloys, and any metal that shows this behavior under cathodic polarization. Moreover, understanding cathodic disintegration in greater detail could allow for the tuning of important parameters such as particle size distribution and surface termination.

## EXPERIMENTAL SECTION

**Materials and Chemicals.** NaOH (>97%), $KHCO_3$ (99.5%), and $H_2SO_4$ (95% solution in water) were purchased from Acros Organics. $Na_2SO_4$ anhydrous (99%), graphite rods (3.05 mm diameter and 38.10 mm long 99.9995%), lead foil (0.76 mm thick 99.8%), tin foil (1 mm thick 99.8%), and high purity Sn and Pb wires (1 mm diameter, 99.998% trace metal basis) were obtained from Alfa Aesar. Sn50Pb50 (wt %) wire (3 mm diameter) was purchased from Merway Inc. Nafion 5 wt % solution in lower aliphatic alcohols and water (15−20% water content) was purchased from Aldrich. $NaNO_3$ (>99%), $NaH_2PO_4$ anhydrous (>99%), $SnCl_2{\cdot}2H_2O$, poly(vinylpirrolidone) (PVP) (MW 55 000), ethylene glycol (EG), $NaBH_4$ (99.99%), and trisodium citrate dihydrate (>99%) were obtained from Sigma-Aldrich. Diamond polishing paste (1 $\mu$m) was obtained from Kemet Europe BV. Carbon cloth 60% Teflon treated and Teflon dispersion DISP 30 were purchased from Fuel Cell Store. An acetylene black powder 75% was obtained from Soltex. Vulcan carbon (VXC72R) was purchased from Cabot Corp. All of the aqueous solutions were prepared using deionized water with a resistivity of 18.2 MΩ cm. All of the chemicals were used as received without further purification.

**Particle Production.** Metal electrodes were polished with a diamond paste, degreased with acetone, rinsed with ultrapure water, and then sonicated for 10 min in ultrapure water. The electrodes were then weighed prior to the experiment.

The disintegration was carried out in a two-electrode undivided cell filled with a 0.3 M $Na_2SO_4$ electrolyte solution and a graphite rod as a counter electrode to minimize the possible contaminations arising from the high anodic potential reached by the counter electrode. During the disintegration process, the cell was placed in a sonication bath to improve the dispersion of the particles coming off of the electrode into the electrolyte. A voltage of 20.5 V was applied with a power supply between the anode and the cathode, which induced the disintegration of the cathode as well as vigorous gas evolution. In the case of Sn and Sn50Pb50, the whole process took about 15 min. In the case of Pb, the reaction was very quick and the plate was disintegrated in 1.5 min at 20.5 V. After the reaction, the electrodes were weighed again to estimate the mass lost during the reaction. Even though the disintegration of the wire became visible at around 4 V for Pb and 6 V for Sn in this electrolyte, the reaction was ultimately carried out at a higher voltage in order for it to be as quick as possible.

The resulting suspension was centrifuged at 10 000 rpm for 10 min. The clear supernatant was discarded and the sediment was resuspended in ethanol, sonicated to disperse it in the solvent, and centrifuged again in the same way. After this last centrifugation step, ethanol was added to the sediment in each tube and the suspension was sonicated for 15 min. Nafion 5 wt % (280 $\mu$L) was added to the resulting suspension and stirred vigorously for at least 1.5 h.

In the case of the Sn/C catalysts, the same process was used but using a 0.1 M NaOH solution instead of 0.3 M $Na_2SO_4$. A high purity Sn wire was immersed by 1.5 cm in the electrolyte solution containing 200 mg of Vulcan carbon and disintegrated. With these quantities, we aimed at producing 30 wt % Sn/C catalysts. We applied a current of 0.5, 0.7, 1, and 1.2 A while continuously stirring the solution until the wire was completely disintegrated, thus opening the circuit. When the disintegration was over, the suspensions were simply filtered with a pressure filter and a hydrophilic PTFE membrane with a pore size of 100 nm and rinsed with MilliQ ultrapure water.

For the benchmark catalyst, we used a previously described chemical reduction method for the production of Sn/C nanoparticles that were used on GDEs in similar conditions.[9] We dissolved 500 mg of $SnCl_2{\cdot}2H_2O$ and 150 mg of poly(vinylpyrrolidone) (PVP) in 100 mL of ethylene glycol (EG). After the dissolution, we added 600 mg of Vulcan carbon (to obtain 30 wt % Sn/C) and used alternated stirring and sonication to obtain a homogeneous dispersion. At this point, 500 mg of $NaBH_4$ was added directly to the solution, which was allowed to react for 30 min. At the end of the reaction, the catalyst was centrifuged and washed with acetone at least three times before drying overnight.

All of the inks based on the Sn/C catalysts were prepared by dissolving the catalyst powder in isopropanol with an amount of 5 wt % Nafion corresponding to a dry 20 wt % of the catalyst.

The catalyst-coated gas diffusion electrodes (GDEs) were prepared by airbrushing the catalytic ink on a strip of the bare GDE prepared by following a previously described method.[10] The metal loading was calculated by the difference in the weight of the electrode before and after airbrushing and assuming that the ratio of a metal to an ionomer was retained during the airbrushing process. The results are shown in Table 1.

**Table 1. Summary of the Metal Loadings on the Prepared GDEs**

| catalyst | metal loading (mg/cm$^2$) |
|---|---|
| Sn | 0.20 |
| Pb | 0.15 |
| Sn50Pb50 | 0.23 |
| Sn/C (0.5 A) | 0.24 |
| Sn/C (0.7 A) | 0.31 |
| Sn/C (1 A) | 0.30 |
| Sn/C (1.2 A) | 0.28 |
| Sn/C chem. red. | 0.27 |

**Particles and Surface Characterization.** X-ray diffraction (XRD) patterns of the unsupported particles were obtained by a Philips X'pert equipped with X'lerator in a 2$\theta$ range from 30 to 80°. Twenty microliters of the particles suspended in ethanol was dropcast on a zero-background quartz stage and analyzed in a diffractometer. The diffractograms of the same metal foils used for disintegration were also obtained for comparison.

Scanning electron microscopy (SEM) was performed on an Apreo SEM equipped with an energy-dispersive X-ray (EDX) analyzer. EDX was used to determine the atomic ratios of Sn and Pb in different areas of the Sn50Pb50 metal foil and the relative particles on the GDE; this way, we could obtain local particle compositional information (within the interaction volume limit of SEM-EDX of about 1 $\mu$m). EDX analysis was also used to investigate the distribution of Sn on the Sn/C powder and estimate the Sn loading on the carbon support.

Transmission electron microscopy (TEM) images were taken in bright-field mode on an FEI Tecnai 20 (type Sphera) operated with a $LaB_6$ filament at 200 kV with a bottom-mounted CETA II 4k × 4k CMOS camera.

**Flow Cell Electrolysis.** The controlled potential electrolysis was carried out in a commercial two-compartment, 10 cm$^2$ GDE flow cell (ElectroCell Micro Flow Cell). The anode and the cathode were separated by a reinforced Nafion membrane N324. The anolyte was a 0.5 M $H_2SO_4$ solution, the anode catalyst was a Ti mesh coated with Ir/$RuO_2$, and the anodic reaction was the oxygen evolution reaction


https://dx.doi.org/10.1021/acssuschemeng.0c04875
ACS Sustainable Chem. Eng. 2020, 8, 15603−15610

(OER). The catholyte was a 0.5 M $KHCO_3$ solution and the cathode was a Sn, Pb, Sn50Pb50, or Sn/C airbrushed GDE. A modified frame in the cathodic compartment allowed for the insertion of a leak-free Ag/AgCl reference electrode close to the surface of the GDE. The electrolyte solutions were circulated in the compartments at a flow rate of 50 mL/min with a peristaltic pump, and $CO_2$ was fed through the GDE in the cathodic compartment at a flow rate of 50 mL/min.

For the testing of the unsupported catalysts, the flow cell was connected to an Autolab PGSTAT100N potentiostat (with Nova software version 1.11) equipped with a 10 A current booster (Autolab BOOSTER10A). The cell was run controlling the potential of the cathode sequentially at −2.44, −1.94, and −2.94 V vs SHE for 1 h.

For the testing of the Sn/C catalysts (synthesized with cathodic disintegration as well as the benchmark), the same apparatus was used but the cell was simply connected to a power supply and operated at 200 $mA/cm^2$ for 4 h.

The samples of the catholyte were collected and analyzed for soluble products with a Metrohm 930 Compact IC Flex ion chromatograph equipped with a Metrohm Metrosep A Supp 7 4 × 250 mm column and a conductivity detector.

## RESULTS

**Disintegration Screening for Catalyst Production.** A voltage of up to 20.5 V was applied between a graphite rod and Sn or Pb electrodes in different electrolytes to screen whether or not the disintegration happened and to assess the stability of the particles in suspension. The results are shown in Table 2.

**Table 2. Summary of the Cathodic Disintegration Behavior in Different Electrolytes for Pb and Sn Foils**

| electrolyte | behavior of cathode | behavior of suspension |
|---|---|---|
| 1 M NaOH | disintegrates | agglomerates |
| 0.1 M NaOH | disintegrates | agglomerates |
| 0.3 M $Na_3$citrate | disintegrates | agglomerates |
| 0.3 M $Na_2SO_4$ | disintegrates | stable |
| 0.3 M $NaH_2PO_4$ | disintegrates | agglomerates |
| 1 M $NaNO_3$ | no disintegration | |
| 0.5 M $H_2SO_4$ | no disintegration | |

As can be seen from the table, the reaction happens in the majority of the electrolytes tested: it is possible to disintegrate Sn and Pb cathodes to a suspension of metallic particles in 1 and 0.1 M NaOH, 0.3 M trisodium citrate, 0.3 M $Na_2SO_4$, and 0.3 M $NaH_2PO_4$ but not in 0.5 M $H_2SO_4$ and 1 M $NaNO_3$. The resulting suspension, with the exception of 0.3 M $Na_2SO_4$, starts to flocculate and bigger particles appear and deposit on the bottom of the container.

Due to the stability of the particles in $Na_2SO_4$, this electrolyte was chosen for the subsequent synthesis of unsupported Sn, Pb, and Sn50Pb50 particles.

In the case of the carbon-supported Sn particles, a 0.1 M NaOH solution was used since the disintegration proceeds more quickly than in $Na_2SO_4$. Also, since Sn is expected to be in situ supported on the carbon present in the electrolyte, the requirement of keeping the suspension stable to prevent the agglomeration of the metallic particles is less stringent.

**Characterization of Disintegration Products.** Figures 1a−c shows a comparison between the XRD patterns of the metal foils used for the disintegration and the unsupported particles obtained from them. Figure 1d shows the results of the EDX analysis performed on the Sn50Pb50 foil and particles to compare the elemental compositions. The foils of pure Sn and Pb are characterized by a distribution of crystallite orientations, as shown in Figure 1a,b, indicating their polycrystalline nature. The particles are at least partly crystalline (we cannot exclude the presence of an amorphous phase) and the peaks do not show significant broadening, suggesting that the crystallite size is rather big. The Sn50Pb50 alloy, according to the phase diagram, should result in a hypoeutectic composition, leading to the formation of a lamellar structure of an $\alpha$ phase (Pb-rich solid solution) and a $\beta$ phase (Sn-rich solid solution) with inclusions of $\alpha$ phase particles. Peaks from Sn and Pb are visible in the diffractogram of both foil and particles (Figure 1c). The peaks are shifted with respect to their position in the pure metals, indicating that Sn and Pb form solid solution phases, as expected. The

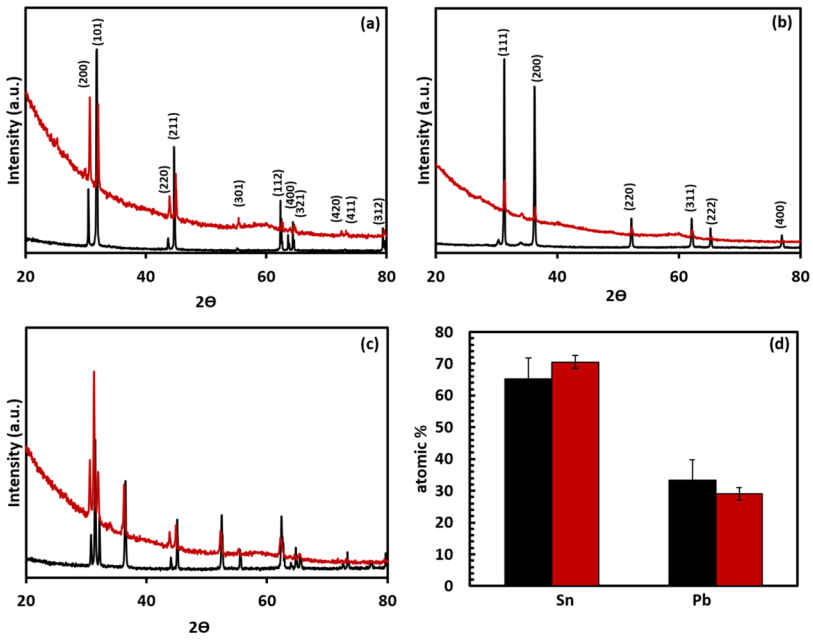


**Figure 1.** Comparison of the XRD foil (black) and particles (red) for (a) Sn, (b) Pb, and (c) Sn50Pb50. (d) Comparison of at. % of Sn and Pb from EDX in the Sn50Pb50 (Sn64Pb36 in at. %) foil (black) and particles (red).



https://dx.doi.org/10.1021/acssuschemeng.0c04875
ACS Sustainable Chem. Eng. 2020, 8, 15603−15610

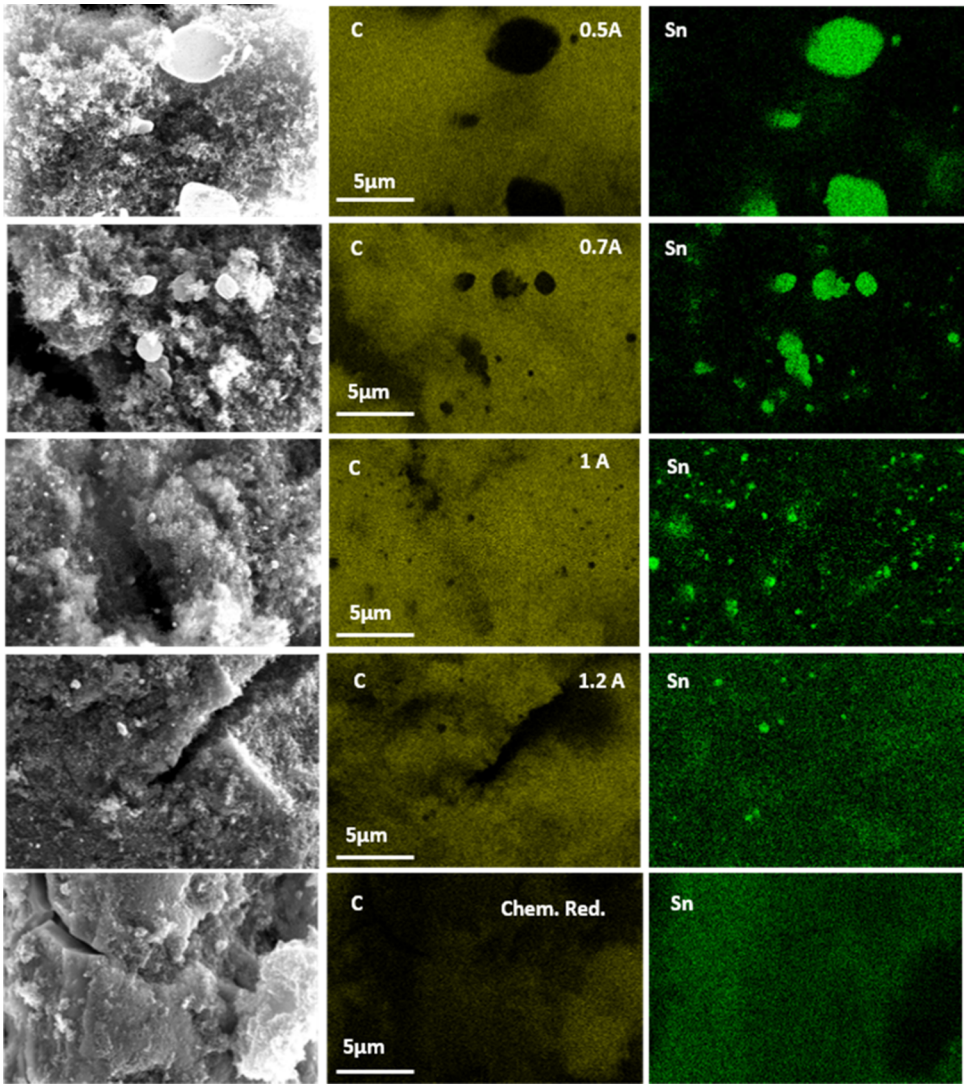


**Figure 2.** EDX elemental mapping of the catalysts produced with cathodic disintegration at different currents. Higher applied currents lead to a better distribution of the catalyst. Probably only beyond a certain threshold current density, most particles are small enough to be effectively supported on the carbon. The catalyst produced by chemical reduction presents the best distribution of Sn on the carbon support.

particles of Sn50Pb50 show a small shift compared to the parent foil, suggesting that some changes in the composition of the Sn−Pb solid solutions might occur during disintegration. The EDX analysis of the Sn50Pb50 metal foil and the corresponding particles shows that the values of atomic composition are mostly retained locally in the alloy particles.

The morphology and size of the unsupported particles were investigated by SEM. As the particles were used for $CO_2$ electrochemical reduction on a GDE-type electrode, the images were taken on the GDE itself and also used to analyze the catalyst distribution on the electrode surface. Some of the SEM pictures taken on the GDEs catalyzed with the unsupported Sn, Pb, and Sn50Pb50 particles are shown in Figure S1. The particle size and shape distribution are very broad, ranging from about 100 nm to micrometers (at least the observed ones). This is probably caused by partial agglomeration of the particles due to the absence of carbon supports or stabilizers. Even though the particles remain in suspension for a longer time in $Na_2SO_4$ (compared to the other electrolytes tested, in which the agglomeration is visible minutes after the end of the disintegration reaction), it does not mean that agglomeration can be entirely prevented. The bigger particles could result from a concomitant mechanical disintegration due to the partial dissolution of the electrode and intense gas evolution.

Interestingly, in the case of carbon-supported Sn particles produced with the disintegration method, we find a correlation between the current applied for the synthesis and the particle size, which in turn influences the efficiency of the support of the Sn particles on the Vulcan carbon. Figure 2 shows SEM-EDX mapping of the catalysts synthesized at the different currents, all at the same magnification and compared to the catalyst synthesized by chemical reduction. At the lowest current (0.5 A), we observe big pieces of Sn (order of 5 $\mu$m) on the carbon support, which are obviously too big to be supported. Moreover, there is a very inhomogeneous and sporadic distribution of Sn on the carbon. The situation becomes better at 0.7 A, but only on increasing the current to 1 A and especially to 1.2 A is the Sn properly distributed on the carbon support in the form of nanoparticles. As we will see later, this impacts the performance of the catalysts. Moreover, the EDX analysis (Figure S2) reveals that the Sn loading on


https://dx.doi.org/10.1021/acssuschemeng.0c04875
ACS Sustainable Chem. Eng. 2020, 8, 15603−15610

the Sn/C catalysts increases with increasing applied current, probably due to the inefficient support of the bigger particles produced at lower currents. These loose particles may be lost during the cleaning procedure. Sn/C 0.5 A, Sn/C 0.7 A, and Sn/C 1 A have Sn loadings lower than the expected 30 wt % (19.6, 19.4, and 26.5%, respectively), while Sn/C 1.2 A and Sn/C chem. red. have a loading slightly higher than the expected value (38.7 and 41.1%, respectively), which may be due to the loss of some of the carbon before particle deposition. Sn/C 1.2 A and Sn/C chem. red. have similar Sn loadings. In any case, since the loading is similar to the expected one, the results of the EDX analysis suggest that the majority of the disintegrated Sn is effectively transformed into particles and there is not a significant loss of Sn as soluble species. In the TEM images, it is difficult to find supported Sn particles in the catalysts synthesized at the lower currents, and in the case of the catalyst synthesized at 0.5 A, it is possible to see big pieces of Sn, thick enough to block the electron beam. In the case of the Sn/C 1.2 A, we can see clusters of nanoparticles on the carbon support (Figure 3). On the

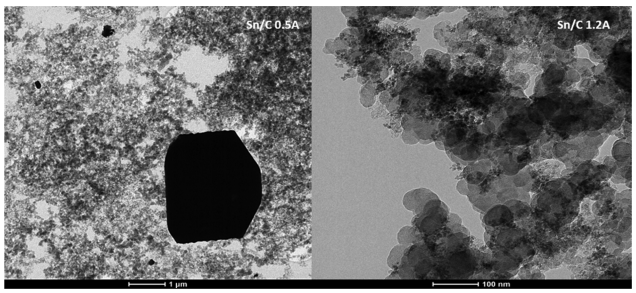


**Figure 3.** TEM images of the Sn/C 0.5 A and Sn/C 1.2 A catalysts. For Sn/C 0.5 A, we find large Sn particles blocking the electron beam and for Sn/C 1.2 A, we can see a homogeneous distribution of Sn nanoparticles clusters on the carbon support.

catalyst produced by chemical reduction, we observe the most homogeneous distribution of Sn on the surface, which is expected as the metal is distributed on and in the pores of the carbon support in the form of soluble $Sn^{2+}$ before being reduced (Figure 2).

**Catalytic Activity for $CO_2$ Reduction.** Figure 4 shows the geometrical current density of the three unsupported catalysts at three different potentials and the faradic yield (FY) toward formate. Since it is known from the previous literature[5,11] that

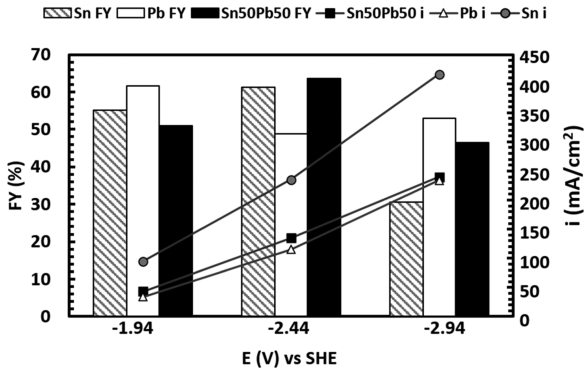


**Figure 4.** Performance of unsupported catalysts in controlled potential flow cell runs: total current densities and faradic yields toward formate for the three catalysts at three different potentials.

Sn, Pb, and Sn−Pb alloys produce formate as a main $CO_2$ reduction product, we did not sample the gas outlet of our electrochemical cell. It is safe to assume that the rest of the current is employed for the evolution of hydrogen and possibly small amounts of CO.

The catalyst reaching the highest partial current toward formate is Sn at a potential of −2.44 V vs SHE with a partial current density of 144 mA/cm$^2$ and FY of about 61%. The most selective catalyst is the Sn50Pb50 alloy at −2.44 V vs SHE with a FY of 64%, however, the total current density is significantly lower for this catalyst, leading to a lower partial current density toward formate of 86 mA/cm$^2$.

For the carbon-supported Sn catalysts produced by cathodic disintegration (results in Figure 5), we can see that the average

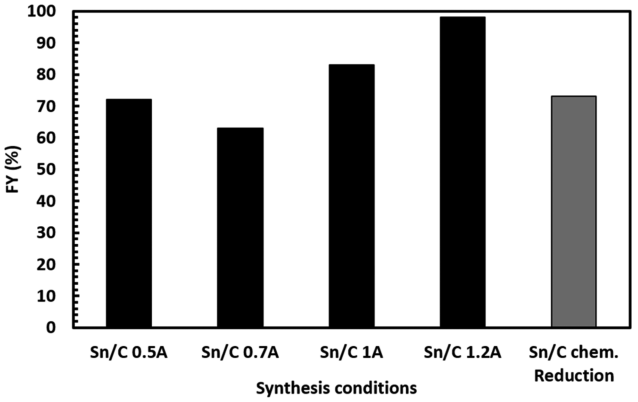


**Figure 5.** Average FY over 4 h at 200 mA/cm$^2$ of the Sn/C catalysts produced with the disintegration method compared to the performance in the same conditions of the Sn/C catalyst prepared by chemical reduction.

FY over 4 h is correlated with the quality of the catalyst distribution on the support. For the Sn/C 0.5 A and the Sn/C 0.7 A catalysts, the FY is, respectively, 72 and 63%, and this is probably due to the fact that the majority of the Sn is not properly supported but exists in the form of micrometric particles, loosely held in the carbon by the binder. We cannot exclude that a fraction of these particles sediments out of the ink during airbrushing. For Sn/C 1 A, we have a higher FY of 83%, while the Sn/C 1.2 A, which is the one that shows the best catalyst distribution in the EDX mappings, is the best one with a FY of 98%. The gray column shows the comparison with the benchmark Sn/C catalyst synthesized by chemical reduction. Sn/C 1 A and Sn/C 1.2 A outperform the benchmark prepared by chemical reduction regarding the selectivity toward formate.

## DISCUSSION

**Particle Formation Mechanism.** As previously discussed in the Results section, it is possible to disintegrate Sn, Pb, and Sn50Pb50 wires in a variety of electrolytes. This phenomenon was first described as cathodic disintegration of Sn and Pb in the 1950s.[6,7] In those papers, the authors explained the process as formation and immediate decomposition of volatile Sn and Pb hydrides upon cathodic polarization.

A more recent explanation for the phenomenon involves the generation of Zintl phases. These are anions based on negatively charged clusters of post transition metals and are known to be extremely unstable.[12] The electrochemical formation of these species is documented for Sn and Pb in


https://dx.doi.org/10.1021/acssuschemeng.0c04875
ACS Sustainable Chem. Eng. 2020, 8, 15603−15610

an anhydrous aprotic organic solvent, in which they can be kept stable for some time by choosing the proper counter ion and keeping strictly anhydrous, anaerobic conditions. Subsequent addition of water to the solvent in which the Zintls are synthesized and stabilized causes the oxidation of the Zintl phase to particles of metallic Sn or Pb.[13] In our case, the formation and decomposition of the Zintl phase (some form of sodium stannide or plumbide) could be happening in a rapid sequence due to the presence of water and lead to the observed disintegration.

A similar process is observed on transition metals and is referred to as cathodic corrosion,[14] which has been suggested to have (ternary metal) hydrides as intermediates.[15] It has been shown that, for this process, it is possible to have some control over particle size distribution and orientation.[16,17] In our case, we know that below a certain threshold current, the particles produced are not supported properly on the carbon because of the formation of large particles in the micrometer range, but we still do not know how variations in the current density above that threshold can create properly supported particles of different sizes and how different electrolytes can influence the process. Most interestingly, there is abundant evidence of the possibility to reliably retain alloy composition of the parent wire in the nanoparticles in the case of cathodic corrosion with an alternating current.[18,19] For now, we have evidence of the possibility to retain alloy composition in a single Sn−Pb alloy but more Sn−Pb alloys and Sn and Pb alloys with other elements can be screened, potentially yielding more selective or stable catalysts.

At this stage, it is still not entirely clear whether cathodic corrosion (transition metals) and cathodic disintegration (Sn and Pb), although similar, are the same phenomenon since they show a different rate dependence on electrolyte concentration and the disintegration of Sn and Pb happens easily in dilute electrolytes with direct currents, while the corrosion of transition metals requires either very concentrated electrolytes with direct current or less concentrated electrolytes with an alternating current.[6,7,14,16−18]

**Control over Particle Size for Supported Sn Particles.** Sn particles of decreasing size can be obtained by increasing the current density applied. This can be observed by comparing the EDX elemental mapping of the carbon-supported catalysts (Figure 2). The reasons for this behavior are not clear, but a possible explanation is that at the lower current densities, the corrosion process is slower and localized in areas of higher mechanical stress (for example, grain boundaries), causing a slow production of nanoparticles and a weakening of the structure, leading to the detachment of the observed larger particles for mechanical instabilities. At higher current densities, instead, the corrosion could happen more homogeneously on the surface, producing significant amounts of nanoparticles small enough to be supported on the carbon (the particle size of Vulcan carbon is between 30 and 60 nm). Some evidence for this behavior is provided by the fact that on disintegrating Sn wires in 0.1 M NaOH at different current densities but passing the same amount of charge, the weight loss increases with increasing current density (see Table S1). This suggests that the process becomes more efficient at higher current densities. In contrast to Sn, we note that for Pt, cathodic corrosion at higher currents leads to larger particles.[16]

**Catalytic Performance.** The values for the FY of the unsupported pure metal catalysts are in line with the previous literature using similar conditions.[11] The significant agglomeration observed in the unsupported catalysts prepared with disintegration makes their performance unsatisfactory for industrial applications. Therefore, since Sn was found to be the better performing catalyst in this study (and also due to the toxicity of Pb), it is interesting to see the effect of dispersing Sn on a carbon support to improve its performance.

The best performing Sn/C catalyst is the Sn/C produced at 1.2 A with an average FY for formate of 98% over 4 h of operation at 200 mA/cm$^2$. This result is significantly better than that of the benchmark catalyst prepared by chemical reduction (73%) in the same conditions despite similar metal loadings on the carbon support. The reasons for this can be multiple. The surface of the particles produced by disintegration could be cleaner due to the absence of organic solvents and polymeric stabilizers. In addition to this, more Sn could be available on the surface of the carbon support in the case of the Sn/C catalyst produced with cathodic disintegration. In catalyst synthesis through chemical reduction, when a metal salt is impregnated into a carbon support and then reduced, a significant fraction of the metal ions could diffuse into the less accessible pores and be reduced directly in there, creating a more homogeneous distribution of metal on the support. This is also observed in the elemental mapping when comparing the catalyst produced by chemical reduction to the ones produced by cathodic disintegration (see Figure 2). Our particles are produced first and then supported, therefore, they may be too big to make it inside the smaller pores of the carbon particles. This creates a higher loading on the most accessible parts of the support. This can be an advantage for reactions that do not require many intermediates to react further (for example, $CO_2$ reduction to formate) but a disadvantage for reactions where the reactants and intermediates need to stay longer near the catalyst sites.[8,20]

**Sustainability.** Cathodic disintegration is likely to have a much higher atom efficiency than conventional chemical reduction methods for catalyst synthesis and generates a considerably lower amount of waste. For a quick comparison: the atom efficiency of the chemical reduction method for the production of Sn/C chem. red. in this paper is 31.8%, while for cathodic disintegration of Sn on the carbon support, assuming the Zintl phase route, we obtain a value of 96.7% (for the calculations, see the Supporting Information). The electrolyte solvent can be reutilized after filtration of the carbon-supported catalyst and the only real waste is the water used to rinse the catalyst after filtration, as opposed to generating an ethylene glycol and acetone stream with residual stabilizer and salts in the case of chemical reduction. In the case of the cathodic disintegration synthesis, the faradic yield for the particle formation is probably low but with only $H_2$ and $O_2$ as byproducts, the use of a dilute aqueous electrolyte as a solvent and the possibility to drive the reaction with renewable energy, this route presents clear environmental advantages. Also, despite the high current density and relatively high voltages needed to drive the reaction, the process happens in a matter of minutes (see Table S2), resulting in low electric power utilization. This makes our method a cheap and sustainable alternative to other chemical reduction−deposition methods. In this study, we did not assess the yield of production, defined as the difference in the weight between the starting materials (Sn + C) and the recovered catalyst. This was decided due to the inefficiency of common laboratory-scale separation techniques used for the recovery of catalyst materials, such as centrifugation and filtration, where a significant fraction of


https://dx.doi.org/10.1021/acssuschemeng.0c04875
ACS Sustainable Chem. Eng. 2020, 8, 15603−15610

materials can be lost in the process. Nevertheless, the EDX analysis shows efficient support of Sn on C in the best conditions, suggesting that the majority of the disintegrated Sn ends in the final product. It is likely that a simple optimization of the separation step will allow for high recovery of the final Sn/C product.

## CONCLUSIONS

We have shown that it is possible to generate catalytically active metallic powders based on Sn and Pb starting from a metallic plate or a wire by cathodic polarization in an appropriate electrolyte. It is also possible to produce a catalyst based on an alloy of Sn and Pb, retaining the composition of the parent wire. The process goes through the disintegration of the cathode and is extremely quick and clean, giving stable suspensions just by carefully choosing the nature and concentration of the electrolyte. This avoids the use of organic solvents, additives, stabilizers, and reducing agents.

The catalysts produced are selective for $CO_2$ reduction to formate at high current densities in a 10 $cm^2$ GDE-type flow cell, with the best performing catalyst being Sn, reaching maximum partial current densities toward formate of 144 mA/$cm^2$ with a faradic yield of 61%.

The catalysts can significantly improve their performance by being properly supported on carbon. The best performing Sn/C catalyst produced with disintegration shows a faradic yield of 98% at 200 mA/$cm^2$, showing promise to be used in industrial electrolyzers.

We are confident that careful optimization of our method of electrochemical particle production can yield catalysts with very good performances that can be produced easily, quickly, and in a clean way. Our method holds promise to be easily scalable to produce large quantities of the catalyst needed for the industrialization of the process of electrochemical conversion of $CO_2$ to formate as well as other (electro)-chemical conversions. We believe that the electrochemically driven production of nanoparticles, both from Sn and Pb as reported here as well as from transition metals as reported in the literature, is an environmentally friendly and promising alternative to conventional catalyst synthesis. The extension of the cathodic disintegration method to other p-block metals remains to be thoroughly investigated. Preliminary results suggest that a similar macroscopically observable process occurs for Bi but no visible disintegration is observed for In, at least in the range of conditions tested. In this case, it may be interesting to investigate the behavior of these metals under conditions similar to the ones that allow the cathodic corrosion of transition metals.

## ASSOCIATED CONTENT

### Supporting Information

The Supporting Information is available free of charge at https://pubs.acs.org/doi/10.1021/acssuschemeng.0c04875.

SEM pictures of unsupported catalysts on GDE, Sn loadings on C estimated with EDX, the weight loss of a Sn wire as a function of the applied current, the summary of synthesis conditions for Sn/C catalysts, and the calculation of atom efficiency for the synthesis of Sn/C catalysts (PDF)

## AUTHOR INFORMATION


### Corresponding Authors

**Davide Pavesi** − *Avantium Chemicals BV, 1014 BV Amsterdam, The Netherlands; Leiden Institute of Chemistry, Leiden University, 2300 RA Leiden, The Netherlands;* orcid.org/0000-0002-3204-4580; Email: davide.pavesi@avantium.com

**Klaas Jan P. Schouten** − *Avantium Chemicals BV, 1014 BV Amsterdam, The Netherlands; Van 't Hoff Institute for Molecular Sciences, University of Amsterdam, 1090 GD Amsterdam, The Netherlands*; Email: KlaasJan.Schouten@avantium.com

### Authors

**Rim C. J. van de Poll** − *Inorganic Materials and Catalysis, Eindhoven University of Technology, 5600 MB Eindhoven, The Netherlands*

**Julia L. Krasovic** − *Avantium Chemicals BV, 1014 BV Amsterdam, The Netherlands*

**Marta Figueiredo** − *Inorganic Materials and Catalysis, Eindhoven University of Technology, 5600 MB Eindhoven, The Netherlands*

**Gert-Jan M. Gruter** − *Avantium Chemicals BV, 1014 BV Amsterdam, The Netherlands; Van 't Hoff Institute for Molecular Sciences, University of Amsterdam, 1090 GD Amsterdam, The Netherlands*

**Marc T. M. Koper** − *Leiden Institute of Chemistry, Leiden University, 2300 RA Leiden, The Netherlands;* orcid.org/0000-0001-6777-4594

Complete contact information is available at: https://pubs.acs.org/10.1021/acssuschemeng.0c04875


### Notes

The authors declare no competing financial interest.

## ACKNOWLEDGMENTS

This research is supported by the European Commission (Research Executive Agency) grant Elcorel (Nr 722614) under the Marie Sklodowska-Curie Innovative Trainings Network.

## REFERENCES


(1) Seh, Z. W.; Kibsgaard, J.; Dickens, C. F.; Chorkendorff, I.; Nørskov, J. K.; Jaramillo, T. F. Combining theory and experiment in electrocatalysis: Insights into materials design. *Science* **2017**, *355*, No. eaad4998.

(2) Lu, X.; Leung, D. Y. C.; Wang, H.; Leung, M. K. H.; Xuan, J. Electrochemical Reduction of Carbon Dioxide to Formic Acid. *ChemElectroChem* **2014**, *1*, 836−849.

(3) Boswell, M. C.; Dickson, J. V. The action of sodium hydroxide on carbon monoxide, sodium formate and sodium oxalate. *J. Am. Chem. Soc.* **1918**, *40*, 1779−178.

(4) Meisel, T.; Halmos, Z.; Seybold, K.; Pungor, E. The thermal decomposition of alkali metal formates. *J. Therm. Anal.* **1975**, *7*, 73−80.

(5) Hori, Y. Electrochemical $CO_2$ Reduction on Metal Electrodes. In *Modern Aspects of Electrochemistry*; Springer: New York, 2008; Vol. *42*, pp 89−189.

(6) Salzberg, H. W. Cathodic Lead Disintegration and Hydride Formation. *J. Electrochem. Soc.* **1953**, *100*, 146−151.

(7) Salzberg, H. W.; Mies, F. Cathodic Disintegration of Tin. *J. Electrochem. Soc.* **1958**, *105*, 64−66.

(8) Witte, P. T.; Berben, P. H.; Boland, S.; Boymans, E. H.; Vogt, D.; Geus, J. W.; Donkervoort, J. G. BASF NanoSelect Technology:

Innovative Supported Pd- and Pt-based Catalysts for Selective Hydrogenation Reactions. *Top Catal.* **2012**, *55*, 505−511.
(9) Del Castillo, A.; Alvarez-Guerra, M.; Solla-Gullón, J.; Sáez, A.; Montiel, V.; Irabien, A. Sn nanoparticles on gas diffusion electrodes: Synthesis, characterization and use for continuous CO2 electroreduction to formate. *J. $CO_2$ Util.* **2017**, *18*, 222−228.
(10) Gulla, A. F.; Krasovic, J. Gas-Diffusion Electrode. U.S. Patent US2014/0227634 A1.
(11) Choi, S. Y.; Jeong, S. K.; Kim, H. J.; Baek, I. H.; Park, K. T. Electrochemical Reduction of Carbon Dioxide to Formate on Tin−Lead Alloys. *ACS Sustainable Chem. Eng.* **2016**, *4*, 1311−1318.
(12) Scharfe, S.; Kraus, F.; Stegmaier, S.; Schier, A.; Fässler, T. F. Zintl Ions, Cage Compounds, and Intermetalloid Clusters of Group 14 and Group 15 Elements. *Angew. Chem., Int. Ed.* **2011**, *50*, 3630−3670.
(13) Yang, Y.; Qiao, B.; Wu, Z.; Ji, X. Cathodic corrosion: an electrochemical approach to capture Zintl compounds for powder materials. *J. Mater. Chem. A* **2015**, *3*, 5328−5336.
(14) Yanson, A. I.; Rodriguez, P.; Garcia-Araez, N.; Mom, R. V.; Tichelaar, F. D.; Koper, M. T. M. Cathodic Corrosion: A Quick, Clean, and Versatile Method for the Synthesis of Metallic Nanoparticles. *Angew. Chem., Int. Ed.* **2011**, *50*, 6346−6350.
(15) Hersbach, T. J. P.; McCrum, I. T.; Anastasiadou, D.; Wever, R.; Calle-Vallejo, F.; Koper, M. T. M. Alkali Metal Cation Effects in Structuring Pt, Rh, and Au Surfaces through Cathodic Corrosion. *ACS Appl. Mater. Interfaces* **2018**, *10*, 39363−39379.
(16) Yanson, A. I.; Antonov, P. V.; Yanson, Y. I.; Koper, M. T. M. Controlling the size of platinum nanoparticles prepared by cathodic corrosion. *Electrochim. Acta* **2013**, *110*, 796−800.
(17) Yanson, A. I.; Antonov, P. V.; Rodriguez, P.; Koper, M. T. M. Influence of the electrolyte concentration on the size and shape of platinum nanoparticles synthesized by cathodic corrosion. *Electrochim. Acta* **2013**, *112*, 913−918.
(18) Feng, J.; Chen, D.; Sediq, A. S.; Romeijn, S.; Tichelaar, F. D.; Jiskoot, W.; Yang, J.; Koper, M. T. M. Cathodic Corrosion of a Bulk Wire to Nonaggregated Functional Nanocrystals and Nanoalloys. *ACS Appl. Mater. Interfaces* **2018**, *10*, 9532−9540.
(19) Rodriguez, P.; Tichelaar, F. D.; Koper, M. T. M.; Yanson, A. I. Cathodic Corrosion as a Facile and Effective Method To Prepare Clean Metal Alloy Nanoparticles. *J. Am. Chem. Soc.* **2011**, *133*, 17626−17629.
(20) Witte, P. T.; Boland, S.; Kirby, F.; van Maanen, R.; Bleeker, B. F.; de Winter, D. A. M.; Post, J. A.; Geus, J. W.; Berben, P. H. NanoSelect Pd Catalysts: What Causes the High Selectivity of These Supported Colloidal Catalysts in Alkyne Semi-Hydrogenation? *ChemCatChem* **2013**, *5*, 582−587.


https://dx.doi.org/10.1021/acssuschemeng.0c04875
*ACS Sustainable Chem. Eng.* 2020, 8, 15603−15610